NONSPECULAR REFLECTION OF ROTATIONALLY SYMMETRIC GAUSSIAN BEAMS FROM SHAPED FLUID-SOLID INTERFACES

Smaine Zeroug and Leopold B. Felsen
Department of Electrical Engineering / Weber Research Institute
Polytechnic University
Farmingdale, N.Y. 11735

INTRODUCTION

Nonspecular reflection, which occurs when an incident beam is phase matched to a leaky wave, is an important tool for fluid-solid interface diagnostics. A recently developed complex ray analysis for modeling nonspecular reflection of two-dimensional Gaussian sheet beams [1,2] is here extended to account for rotationally symmetric three-dimensional (3D) Gaussian beams (GBs) with arbitrary collimation. As in our 2D analysis, we utilize the complex-source-point (CSP) technique by which a conventional point-source-excited field can be converted into a 3D quasi-Gaussian beam field by displacing a real point source to a complex location [3]. When the CSP field excited in the fluid interacts with a plane or cylindrically layered elastic medium, the resulting internal and external fields can be expressed rigorously in terms of wavenumber spectral integrals that are approximated explicitly by high-frequency uniform asymptotics [4]. The resulting expressions for the reflected field contain interacting specularly reflected beam and leaky wave contributions which establish the physical basis for the observed phenomena.

We have applied this modeling to arbitrarily collimated 3D beams impinging on plane and cylindrically layered geometries, with particular attention to beams meeting the phase matching condition for the leaky Rayleigh wave that can propagate along a fluid-solid interface. It is shown that for phase-matched well collimated beams incident on planar or cylindrical interfaces, the nonspecular reflected field retains essentially the simple features observed for 2D sheet beams [1,2], except that the 3D fields are windowed laterally by a Gaussian envelope. However, diverging beams give rise to more complex reflected patterns owing to the now more extended and nonuniform interaction regions between the specularly reflected and the leaky wave fields. While the entire formulation here accounts for phase matching to only one leaky wave, extension to multiple leaky waves as encountered in layered environments is straightforward.

Review of Progress in Quantitative Nondestructive Evaluation, Vol. 12
Edited by D.O. Thompson and D.E. Chimenti, Plenum Press, New York, 1993

The paper is organized as follows. The analytical foundation for plane and cylindrically layered elastic structures is presented first, with implementation of the CSP method. Asymptotic reductions generate explicitly the incident CSP beam and the corresponding specularly reflected and leaky wave fields. These expressions are then used to compute numerical results for beams with various collimations impinging on planar and cylindrical water-aluminum interfaces, and the results are interpreted physically. Final remarks about the advantages of the complex ray method conclude the presentation.

FORMULATION

We consider 3D scattering of the pressure field $\mathcal{P}$ in the fluid excited by a high-frequency point source in the presence of a plane or cylindrically layered elastic structure. With the source located at $\underline{r}'$, the time-harmonic pressure field $\mathcal{P}$ at an observation point $\underline{r}$ in the fluid can be derived from a displacement potential field Φ,

$$\mathcal{P}(\underline{r},\underline{r}') = -\rho_f \omega^2 \Phi(\underline{r},\underline{r}') \tag{1}$$

where ρ_f is the fluid density, ω is the source frequency and a time dependence $\exp\{-i\omega t\}$ is suppressed. The potential field in the fluid satisfies the source-excited Helmholtz equation with boundary conditions that account for the layered elastic structure, in addition to a radiation condition at infinity. Solution of these boundary value problems is effected in the spectral wavenumber domain corresponding to the space coordinates tangential to the layer boundaries [4]. For the plane layered $\underline{r}=(x,y,z)$ geometry, with the layer interfaces along (x,y) (see Fig.1a), the spectral wavenumbers are denoted by (k_x,k_y) whereas for the cylindrically layered $\underline{r}=(\rho,\phi,z)$ geometry, with the layer interfaces along (ϕ,z) (see Fig.1b), the spectral wavenumbers are (ν,β). With a caret denoting spectral domain quantities, the spectral decomposition yields for the planar and cylindrical cases, respectively,

$$\Phi_{pl}(\underline{r},\underline{r}') = \frac{1}{(2\pi)^2} \int_{-\infty}^{\infty}\int_{-\infty}^{\infty} dk_x dk_y \, \hat{\Phi}(k_x,k_y) \exp\{ik_x(x-x')+ik_y(y-y')\} \tag{2a}$$

$$\Phi_{cyl}(\underline{r},\underline{r}') = \frac{1}{(2\pi)^2} \int_{-\infty}^{\infty}\int_{-\infty}^{\infty} d\nu d\beta \, \hat{\Phi}(\nu,\beta) \exp\{i\nu(\phi-\phi')+i\beta(z-z')\} \tag{2b}$$

Note that k_x, k_y, and β have the dimensions of $(\text{length})^{-1}$ while ν is dimensionless. The reduced forms of the wave equations for the planar and cylindrical cases can be solved to yield [4]

$$\hat{\Phi}_{pl}(k_x,k_y) = \frac{i}{2\kappa_f}\left[\exp\{i\kappa_f|z-z'|\} + R(k_x,k_y)\exp\{-i\kappa_f(z+z')\}\right], \quad z \le 0 \tag{3a}$$

$$\hat{\Phi}_{cyl}(\nu,\beta) = \frac{i\pi}{4}\left\{H_\nu^{(2)}(\kappa_f\rho_<) + R(\nu,\beta)\frac{H_\nu^{(2)}(\kappa_f a)}{H_\nu^{(1)}(\kappa_f a)} H_\nu^{(1)}(\kappa_f\rho_<)\right\} H_\nu^{(1)}(\kappa_f\rho_>); \rho,\rho' > a \tag{3b}$$

$$\kappa_f = \sqrt{k_f^2 - \varsigma^2}\,, \quad \begin{cases} \mathrm{Re}\{\kappa_f\} > 0 \text{ when } |\varsigma| < k_f \\ \mathrm{Im}\{\kappa_f\} > 0 \text{ when } |\varsigma| > k_f \end{cases}, \tag{4}$$

where $\varsigma^2 \equiv k_x^2 + k_y^2$ (planar), $\varsigma \equiv \beta$ (cylindrical), $k_f = \omega/v_f$, v_f is the sound speed in the fluid, and a is the radius of the outermost fluid-solid interface, while $R(k_x,k_y)$ and $R(\nu,\beta)$ are, respectively, the spectral domain reflection coefficients accounting for the scattering from the plane and cylindrically layered environments [5].

Equations (2), (3), and (4) represent the formal solutions for point-source-excited inputs. The total field excited by a beam input can be constructed via the complex-source-point (CSP) technique [3]. With a tilde ˜ denoting a complex coordinate as well as functions of a complex coordinate, the point source is displaced into the complex coordinate plane via

planar: $$x' \to \tilde{x}' = x' + ib\sin\alpha_o\,,\ y' \to \tilde{y}' = y'\,,\ z' \to \tilde{z}' = z' + ib\cos\alpha_o \tag{5}$$

cylindrical:

$$x' \to \tilde{x}' = x' + ib\cos\alpha_z \sin\alpha_\phi\,,\ y' \to \tilde{y}' = y' + ib\cos\alpha_z \cos\alpha_\phi\,,\ z' \to \tilde{z}' = z' + ib\sin\alpha_z \tag{6a}$$

$$\rho' \to \tilde{\rho}' = \sqrt{\tilde{x}'^2 + \tilde{y}'^2}\,, \mathrm{Re}\{\tilde{\rho}'\} \geq 0;\ \phi' \to \tilde{\phi}' = \tan^{-1}\left\{\tilde{x}'/\tilde{y}'\right\} \text{ with } \tilde{\phi}' = \pi \text{ when } \tilde{x}' = 0 \tag{6b}$$

The real-space field radiated by this complex source is a rotationally symmetric three dimensional beam with quasi-Gaussian amplitude profile whose maximum lies along the angular direction α_o for the planar geometry (see Fig.1a), and in the direction defined by α_z and α_ϕ for the cylindrical geometry (see Fig.1b). The 1/e beam width w_o at the waist (x',y',z') is given by $w_o = (2b/k_f)^{1/2}$, which establishes the real parameter b as the Fresnel length of the beam. Note that substitution of the complex extensions (5) and (6) into (2) and (3) yields exact formal solutions for the beam input.

The exact spectral integrals representing Φ in the fluid can be evaluated asymptotically by the saddle point method applied in the complex wavenumber planes. Typically, one deforms the integration contours from the real axes in the complex (k_x,k_y) or (ν,β) planes, along which the integrand is highly oscillatory, into the steepest descent paths (SDPs) passing through the stationary (saddle) points of the phase of the integrand in each plane. The dominant contribution to the high frequency field then arises from the saddle points and from the singularities (poles and branch points) intercepted during the SDP deformations. Nonspecular reflection of bounded beams, which is the concern of this study, is characterized by the strong interaction of the reflected beam field contributed by a saddle point and a leaky wave pole singularity of the spectral reflection coefficient. This strong interaction, generated by phase matching between the incident beam and the leaky wave, manifests itself by the close proximity of the leaky wave pole (subscript p) and the saddle point (subscript s), thereby requiring uniform asymptotics in the reduction of the spectral integrals [4]. For the planar case, it is convenient to carry out the asymptotic evaluation in the auxiliary complex (angular spectrum) k and α planes

defined by $k_x=k\cos\alpha$ and $k_y=k\sin\alpha$. In this case, the final expression for the total asymptotic potential field in the fluid is found to be given by

$$\Phi_{pl}(\underline{r},\underline{r}') \sim \frac{\exp\{ik_f\tilde{L}_t\}}{4\pi\,\tilde{L}_t} + R(\tilde{k}_s)\frac{\exp\{ik_f(\tilde{L}'+\tilde{L})\}}{4\pi(\tilde{L}'+\tilde{L})}$$
$$-\frac{\exp\{-i/4\}}{2\sqrt{2\pi}}\sqrt{\frac{k_p}{(k_f^2-k_p^2)}}\,\frac{N(k_p)}{\partial D(k_p)/\partial k}\frac{1}{\sqrt{\tilde{\rho}}}\exp\left\{i\tilde{P}^r(k_p,\tilde{\alpha}_s)\right\}\mathcal{F}(-i\tilde{s}_p) \quad (7)$$

where

$$\tilde{L}_t=\sqrt{(x-\tilde{x}')^2+(y-\tilde{y}')^2+(z-\tilde{z}')^2}\,,\quad \mathrm{Re}\{\tilde{L}_t\}\geq 0 \quad (7a)$$

while $\tilde{s}_p$ and N, D are defined in (9) and (10), respectively. The leaky wave pole k_p is the solution of $D(k_p)=0$. Moreover,

$$\tilde{P}^r(k,\alpha)=k\cos\alpha\,(x-\tilde{x}')+k\sin\alpha\,(y-\tilde{y}')-\kappa_f(z+\tilde{z}') \quad (7b)$$

$$\tilde{L}'=-\tilde{z}'/\cos\tilde{\theta}_{rs}\,,\ \tilde{L}=-z/\cos\tilde{\theta}_{rs}\,,\ \tilde{\theta}_{rs}=\tan^{-1}\left[\frac{\sqrt{(x-\tilde{x}')^2+(y-\tilde{y}')^2}}{-(z+\tilde{z}')}\right] \quad (7c)$$

$$\tilde{\rho}=\sqrt{(x-\tilde{x}')^2+(y-\tilde{y}')^2}\,,\quad \mathrm{Re}\{\tilde{\rho}\}\geq 0 \quad (7d)$$

$$\mathcal{F}(-i\tilde{s}_p)=\frac{1}{2}erfc(-i\tilde{s}_p)-\frac{\exp\{-(-i\tilde{s}_p)^2\}}{2\sqrt{\pi}\,(-i\tilde{s}_p)}\,,\quad erfc(u)=\frac{2}{\sqrt{\pi}}\int_u^{\infty}\exp\{-t^2\}dt \quad (7e)$$

The complex lengths $\tilde{L}_t$, $\tilde{L}'$ and $\tilde{L}$ are extensions of the distances from the beam waist to the observer measured along the direct path ($\tilde{L}_t$) or along the specularly reflected path segments to ($\tilde{L}'$) and from ($\tilde{L}$) the interface. The saddle point $(\tilde{k}_s,\tilde{\alpha}_s)$ is defined explicitly by

$$\tilde{k}_s=k_f\sin\tilde{\theta}_{rs}\,,\quad \tilde{\alpha}_s=\tan^{-1}[(y-\tilde{y}')/(x-\tilde{x}')] \quad (7f)$$

For the cylindrical case, the Hankel functions in (3b) are approximated by high-frequency Debye asymptotics, and the asymptotic evaluations are performed sequentially in the ν and β planes. The final expression is found to be given by

$$\Phi_{pl}(\underline{r},\underline{r}') \sim \frac{\exp\{ik_f\tilde{L}_t\}}{4\pi\,\tilde{L}_t} + R(\tilde{\nu}_s,\tilde{\beta}_s)\frac{\exp\{ik_f(\tilde{L}'+\tilde{L})\}}{4\pi(\tilde{L}'+\tilde{L})}\sqrt{\frac{a(\tilde{l}'+\tilde{l})\sin\gamma_a}{2\tilde{l}'\tilde{l}+a(\tilde{l}'+\tilde{l})\sin\gamma_a}\Bigg|_{\tilde{\nu}_s,\tilde{\beta}_s}}$$
$$-\frac{1}{4\pi}\left[\frac{N(\nu,\beta)}{\partial D(\nu,\beta)/\partial\nu}\frac{\exp\left\{i\tilde{P}^r(\nu,\beta)\right\}}{\sqrt{(k_f^2-\beta^2)\rho\tilde{\rho}'\sin\gamma\sin\tilde{\gamma}'}}\sqrt{\frac{2\pi i}{d^2\tilde{P}^r(\nu,\beta)/d\beta^2}}\right]_{(\nu_p(\tilde{\beta}_s'),\tilde{\beta}_s')}\mathcal{F}(-i\tilde{s}_p) \quad (8)$$

where

$$\tilde{P}^{\mathcal{I}}(\nu,\beta)=\kappa_f(\rho\sin\gamma+\tilde{\rho}'\sin\tilde{\gamma}'-2a\sin\gamma_a)-\nu(\gamma+\tilde{\gamma}'-2\gamma_a-[\phi-\tilde{\phi}'])+\beta(z-\tilde{z}') \tag{8a}$$

$$\tilde{L}'+\tilde{L}=(\tilde{l}'+\tilde{l})\left(1-\tilde{\beta}_s^2/k_f^2\right)^{1/2}+(z-\tilde{z}')\tilde{\beta}_s/k_f\,,\quad \left\{\begin{matrix}\tilde{l}'=(\tilde{\rho}'\sin\tilde{\gamma}'-a\sin\gamma_a)\\ \tilde{l}=(\rho\sin\gamma-a\sin\gamma_a)\end{matrix}\right\}_{\tilde{\nu}_s,\tilde{\beta}_s} \tag{8b}$$

$$\tilde{\gamma}=\cos^{-1}\left(\tilde{\nu}/\kappa_f\rho\right),\qquad \tilde{\gamma}'=\cos^{-1}\left(\tilde{\nu}/\kappa_f\tilde{\rho}'\right),\qquad \tilde{\gamma}_a=\cos^{-1}\left(\tilde{\nu}/\kappa_f a\right) \tag{8c}$$

The saddle point $(\tilde{\nu}_s,\tilde{\beta}_s)$ is defined by the coupled equations,

$$\left(\gamma+\tilde{\gamma}'-2\gamma_a-\left[\phi-\tilde{\phi}'\right]\right)_{\tilde{\nu}_s,\tilde{\beta}_s}=0 \tag{8c}$$

$$\left(\beta\left[k_f^2-\beta^2\right]^{-1/2}(\rho\sin\gamma+\tilde{\rho}'\sin\tilde{\gamma}'-2a\sin\gamma_a)\right)_{\tilde{\nu}_s,\tilde{\beta}_s}-(z-\tilde{z}')=0 \tag{8d}$$

The leaky wave pole $\left(\nu_p(\tilde{\beta}_s'),\tilde{\beta}_s'\right)$ is defined by

$$D(\nu(\beta),\beta)=0 \text{ and } d\tilde{P}^{\mathcal{I}}(\nu(\beta),\beta)/d\beta\big|_{\nu_p(\tilde{\beta}_s'),\tilde{\beta}_s'}=0 \tag{8e}$$

In the above,

$$\tilde{s}_p=\sqrt{i\left[\tilde{P}^{\mathcal{I}}(\tilde{\varsigma}_s)-\tilde{P}^{\mathcal{I}}(\tilde{\varsigma}_p)\right]}\,,\quad \left\{\begin{matrix}\tilde{\varsigma}_s\equiv(\tilde{k}_s,\tilde{\alpha}_s);\ \tilde{\varsigma}_p\equiv(k_p,\tilde{\alpha}_s)\quad\text{(planar)}\\ \tilde{\varsigma}_s\equiv(\tilde{\nu}_s,\tilde{\beta}_s);\ \tilde{\varsigma}_p\equiv\left(\nu_p(\tilde{\beta}_s'),\tilde{\beta}_s'\right)\ \text{(cylindrical)}\end{matrix}\right. \tag{9}$$

The quantities $N()$ and $D()$ denote the numerator and denominator of the spectral reflection coefficient R() which is approximated by

$$R(\varsigma)=\frac{N(\varsigma)}{D(\varsigma)}=\frac{\varsigma-k_p^*}{\varsigma-k_p}\,,\quad \varsigma\equiv k\ \text{(planar)}\ \text{ or }\ \varsigma\equiv\sqrt{(\nu/a)^2+\beta^2}\ \text{(cylindrical)} \tag{10}$$

with the asterisk expressing the complex conjugate. The commonly used simple form of (10) (see [1,2]) accounts for the relevant spectral phenomena associated with nonspecular reflection, in particular, the main splitting due to the close proximity of a pole and a zero in (10). The first two terms in (7) or (8) represent, respectively, the incident or direct beam field and the specularly reflected beam field. The third term accounts for the 'uniform' leaky wave field. The uniformity of the solution is embedded in the transition function $\mathcal{T}()$ in (7e) which accounts for the strong (leaky wave)-(reflected beam) interaction. When the observer moves outside the strongly interacting nonspecular reflection region, $\mathcal{T}()$ either reduces to unity or vanishes. The former occurs when the pole is intercepted by the deformed contour, and the latter

when it is not. Simultaneous phase matching to multiple leaky waves is accounted for by simple summation of uniform leaky wave fields [5].

NUMERICAL RESULTS

The numerical results below implement (7) and (8) for planar and cylindrical water-aluminum interfaces as shown in Figs.1a and 1b, respectively, under conditions where the incident Gaussian beam is nearly or exactly phase matched to the leaky Rayleigh wave. The leaky wave spectral pole (see (10)) is located at [1,2],

$$k_p = k_p^{\mathrm{r}} + i\, k_p^{\mathrm{i}}; \qquad k_p^{\mathrm{r}} = k_f \sin(30.593^{\circ}), \quad k_p^{\mathrm{i}} = 0.01494\, k_f \tag{11}$$

Surface and contour plots of the field magnitudes on the surface $z=0$ in the plane geometry are shown in Figs.2 and 3. Figure 2 depicts the profiles of well collimated and diverging incident beams, while Fig.3 depicts the profiles of the corresponding nonspecular reflected fields (not including the incident fields). The beam axes are contained in the $y=0$ plane and intersect the $z=0$ plane at $(x=0,y=0)$. It is noted from Fig.3a that the reflected field for the well collimated case is split as well as shifted toward the direction of incidence. In the $y=0$ plane, these features are quite similar to those observed for y-independent 2D beams [2,3]. Out-of-plane 3D effects are accounted for by Gaussian profiling along y. The nearly exponential decay along x for $x>10$ indicates that the leaky wave field is dominant there. The reflected field for the diverging case (Fig.3b) is more complex. The multiple splitting, which also occurs for 2D beams, is due to the more extended region of interaction as well as the beating between the strongly varying periodicities induced on the surface by the specularly reflected portion and the constant periodicity of the leaky wave [1,2]. The interference is strongest in the principal plane $y=0$ (line P in Fig.2b), but diminishes, with more widely spaced interference nulls, away from the principal plane (along lines Q), thereby yielding the arched pattern in Fig.3b.

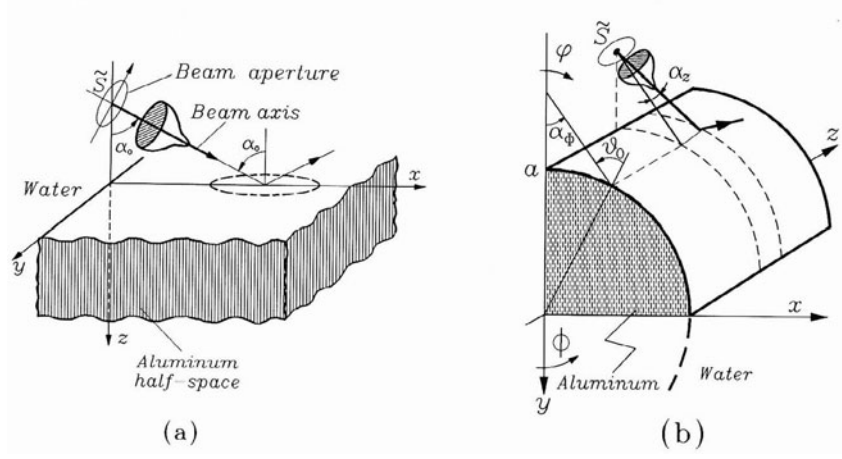

Fig.1 Geometries and coordinates for fluid-solid configurations excited by 3D CSP beams. $\tilde{S}$: CSP beam source with equivalent beam aperture located at (x',y',z'). (a) planar, (b) cylindrical.

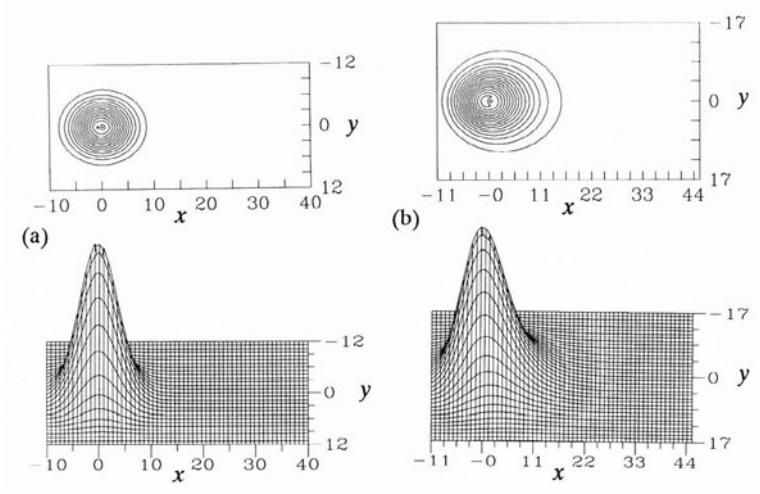

Fig.2 Surface and contour plots of the incident beam field magnitude for (a) a well collimated and (b) a diverging beam observed on a plane interface $z=0$ between water and an aluminum half-space (see Fig.1a). Parameters: $(x',y',z')=(-11.83,0,-20)$, $\alpha_o=30.593^o$, (a) $b=50$; (b) $b=5$. All distances are normalized to the fluid wavelength $\lambda_f=2\pi/k_f$.

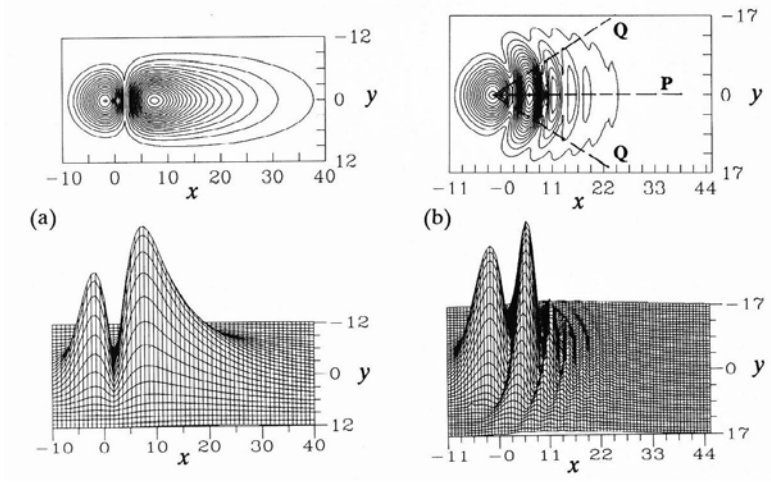

Fig.3 As in Fig.2, but for the corresponding induced reflected fields. Magnitude profiles computed from (7).

Corresponding phenomena induced by a wide well collimated beam on the cylindrical interface $\rho=a$ of Fig.1b are shown in Fig.4. The incident beam axis lies in the $z=0$ plane and intersects the cylinder surface at $(a\varphi,z)=(12.82,0)$. As for 2D beams, curvature changes the well collimated incident beam profile into the diverging profile similar to that in Fig.2b for the planar case. Accordingly, one may note the similarities of the on-surface reflected fields in Figs.3b and 4b, and can interpret the results in Fig.4b by the same interference phenomena as in Fig.3b.

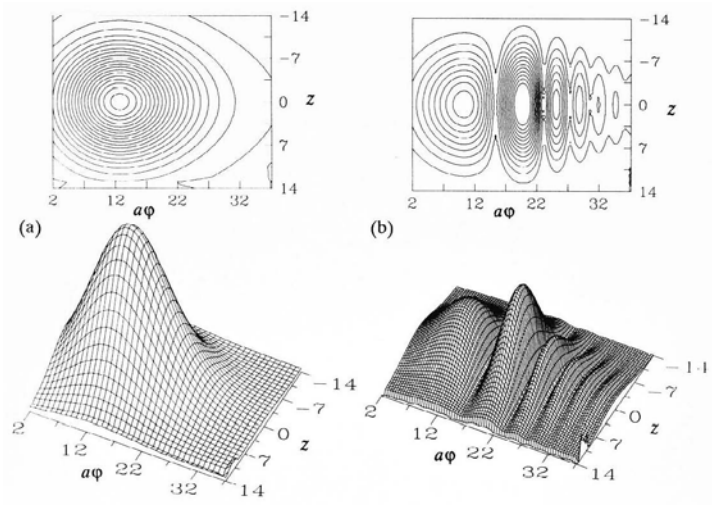

Fig.4 Surface and contour plots of (a) incident and (b) nonspecular reflected field magnitudes for a wide well-collimated beam, observed on the surface $\rho=a$ of a water-immersed aluminum cylinder. Parameters: $(x',y',z')=(10,-50,0)$, $\alpha_\phi=12.22^o$ (corresponding incidence angle on interface: $\theta_0=30.593^o$), $\alpha_z=0^o$, $b=200$, $a=40$. Magnitude profiles computed from (8). All distances are normalized to fluid wavelength.

CONCLUSIONS

The CSP method has been shown to furnish a versatile algorithm for predicting interaction of arbitrarily collimated rotationally symmetric 3D Gaussian beams with plane and cylindrical fluid-solid interfaces, at arbitrary incidence angles that include phase matching to leaky waves. The algorithm can be implemented numerically without difficulty, and can be generalized to arbitrarily curved and layered configurations. Details and extensions will be described in a separate manuscript [5].

ACKNOWLEDGEMENT

This work has been supported in part by the David Taylor Research Center under subcontract from Johns Hopkins University.

REFERENCES

1. S. Zeroug and L. B. Felsen, in *Review of Progress in Quantitative NDE*, Vol. 11, edited by D. O. Thompson and D. E. Chimenti (Plenum Press, NY, 1992), p.129.
2. S. Zeroug and L. B. Felsen, "Nonspecular Reflection of Beams from Liquid-Solid Interfaces," to be published in J. Nondestructive Evaluation, Special Issue on "Modeling and Characterization of Interfaces in QNDE".
3. L. B. Felsen, Geophys. J. R. Astron. Soc. Vol.79, 77-88 (1984).
4. L. B. Felsen and N. Marcuvitz, *Radiation and Scattering of Waves* (Prentice Hall, Englewood Cliffs, N.J., 1973).
5. Manuscript in preparation.